Classical plasma dynamics of Mie-oscillations in atomic clusters

IOP Conf. Series: Journal of Physics: Conf. Series **999** (2018) 012006 doi:10.1088/1742-6596/999/1/012006

Classical plasma dynamics of Mie-oscillations in atomic clusters

H.-J. Kull and A. El-Khawaldeh

Institute for Theory of Statistical Physics, Laser Physics Group, RWTH Aachen University, 52056 Aachen, Germany

E-mail: kull@ilt-extern.fraunhofer.de

Abstract. Mie plasmons are of basic importance for the absorption of laser light by atomic clusters. In this work we first review the classical Rayleigh-theory of a dielectric sphere in an external electric field and Thomson's plum-pudding model applied to atomic clusters. Both approaches allow for elementary discussions of Mie oscillations, however, they also indicate deficiencies in describing the damping mechanisms by electrons crossing the cluster surface. Nonlinear oscillator models have been widely studied to gain an understanding of damping and absorption by outer ionization of the cluster. In the present work, we attempt to address the issue of plasmon relaxation in atomic clusters in more detail based on classical particle simulations. In particular, we wish to study the role of thermal motion on plasmon relaxation, thereby extending nonlinear models of collective single-electron motion. Our simulations are particularly adopted to the regime of classical kinetics in weakly coupled plasmas and to cluster sizes extending the Debye-screening length. It will be illustrated how surface scattering leads to the relaxation of Mie oscillations in the presence of thermal motion and of electron spill-out at the cluster surface. This work is intended to give, from a classical perspective, further insight into recent work on plasmon relaxation in quantum plasmas [1].

1. Introduction

Mie oscillations in atomic clusters are of basic interest in the study of finite-size electronic properties of nanoparticles. The size dependence of the damping constant of Mie oscillations has received much attention and was treated by classical mean free path models [2, 3] and quantum theoretical linear response [4] and random phase approximation calculations [5]. More generally, damping is attributed to collisions, outer ionization [6, 7], surface scattering [16] and radiation emission. In laser excitations damping is often accompanied by linear [8, 9, 10] and nonlinear [11, 12, 13] resonance absorption. In this work we wish to investigate in more detail Mie oscillations and their relaxation by classical particle simulations. For this purpose, the model of a homogeneously charged ion sphere neutralized by N electrons with a soft-core Coulomb interaction is considered. This model has only two dimensionless parameters, the particle number N and the plasma coupling constant Γ. In this work, we consider a weakly coupled plasma with $\Gamma = 0.1$ and clusters in the range of $N = 8000 - 27000$ particles. After a brief introduction to Mie oscillations of clusters and surface scattering within a hollow sphere, the particle simulations are described and results for the size-dependent damping rates are discussed and compared with previous work.

2. Mie-oscillations

2.1. Rayleigh theory

We first review some basic properties of Mie oscillations in atomic clusters. Mie oscillations arise from the polarization of the cluster in an external radiation field. The famous Mie theory treats light scattering by a dielectric sphere of an arbitrary size. If the radius of the sphere is much smaller than the wavelength of the radiation, one can restrict attention to the simpler theory of Rayleigh scattering. As originally demonstrated by Rayleigh, a small sphere with dielectric constant ϵ placed in a uniform electric field $\boldsymbol{E}_0$ acquires a homogeneous polarization ([14], p.32, eq.(20))

$$\boldsymbol{P} = \frac{3}{4\pi}\frac{\epsilon - 1}{\epsilon + 2}\boldsymbol{E}_0. \tag{1}$$

The electric field produced by a homogeneously polarized sphere is given by

$$\boldsymbol{E}_P = -\frac{4\pi}{3}\boldsymbol{P} = -\frac{\epsilon - 1}{\epsilon + 2}\boldsymbol{E}_0 \tag{2}$$

and the total electric field inside the sphere, consisting of the polarization field and the external field, becomes

$$\boldsymbol{E} = \boldsymbol{E}_0 + \boldsymbol{E}_P = \frac{3}{\epsilon + 2}\boldsymbol{E}_0. \tag{3}$$

The electrostatic treatment is still applicable to harmonic fields of frequency ω, if the static dielectric constant is replaced by a frequency-dependent function $\epsilon = \epsilon(\omega)$ and the radius of the sphere is much smaller than the wavelength. The Mie resonance is defined by the condition that the denominator of the electric field (3) becomes zero,

$$\epsilon(\omega) + 2 = 0. \tag{4}$$

At this stage, the Rayleigh theory is purely macroscopic and the Mie-resonance frequencies are just zeros of $\epsilon(\omega) + 2$ for any dielectric function under consideration. As a simple microscopic model, one often chooses a free electron gas with the dielectric function

$$\epsilon(\omega) = 1 - \frac{\omega_p^2}{\omega^2}, \qquad \omega_p^2 = \frac{4\pi e^2 n_0}{m}, \tag{5}$$

where ω_p denotes the plasma frequency, n_0 a homogeneous electron density, e the elementary charge in Gaussian cgs units and m the electron mass. Then the resonance occurs at the well-known Mie frequency

$$\omega_M = \frac{1}{\sqrt{3}}\omega_p. \tag{6}$$

2.2. Thomson model

We now discuss a microscopic model of Mie oscillations in clusters, that is based on the motion of N electrons inside a sphere of radius R with a homogeneous positive charge density en_0. This model is reminiscent of the famous plum-pudding model of Thomson [15], viewing atoms as an extended homogeneous positively charged nucleus and the electrons as point charges immersed into this background. While Thomson's model failed to explain the structure of atoms, it is commonly used as a model of an extended plasma with a neutralizing homogeneous background. The electric field of the homogeneously charged ion sphere with charge density en_0 at a position $\boldsymbol{r}$ inside the sphere is given by

$$\boldsymbol{E}_I(\boldsymbol{r}) = \frac{4\pi}{3}en_0\boldsymbol{r} = \frac{m}{e}\omega_M^2\boldsymbol{r}. \tag{7}$$

Inside the sphere, the motion of electron i is described by

$$m\ddot{\boldsymbol{r}}_i = -e\boldsymbol{E}_I(\boldsymbol{r}_i) + \sum_{j\neq i} \frac{e^2}{|\boldsymbol{r}_i - \boldsymbol{r}_j|^3}(\boldsymbol{r}_i - \boldsymbol{r}_j) - e\boldsymbol{E}_0(t), \qquad i,j = 1,\cdots,N \tag{8}$$

where the first term describes the electron-ion, the second one the electron-electron interaction and the last one an external time-dependent field. Here and in the following parts of this section it is assumed, that electrons move inside the sphere without reaching or crossing its boundary. The equation of motion becomes particularly simple, if one considers the center of mass (c.m.)

$$\boldsymbol{R} = \frac{1}{N}\sum_i \boldsymbol{r}_i \tag{9}$$

of all electrons. In this case, (8) has to be averaged over all electrons. For the average of the force one can draw three important conclusions:

(i) Due to the action-reaction law, the electron-electron interactions cancel. The electrons therefore exert no force on the c.m.

(ii) For an isotropic electron distribution, the electron-ion interaction will also vanish for any central field $\boldsymbol{E}_I = -\nabla\phi(r)$ that can be derived from an arbitrary spherically symmetric potential $\phi(r)$. Accordingly, in equilibrium, the c.m. will be assumed force-free and coincident with the center of the ion sphere.

(iii) The average force becomes particularly simple for spatially constant and linear forces. Assuming a force $\boldsymbol{f}(\boldsymbol{r}) = -k\boldsymbol{r} + \boldsymbol{f}_0$ with constants k and $\boldsymbol{f}_0$ acting on the particles at positions $\boldsymbol{r}_i$, the ensemble average will be given by

$$\boldsymbol{F} = \frac{1}{N}\sum_i \boldsymbol{f}(\boldsymbol{r}_i) = -k\boldsymbol{R} + \boldsymbol{f}_0 = \boldsymbol{f}(\boldsymbol{R}).$$

As in the quantum-mechanical Ehrenfest-theorem, the average can be moved in this special case from the force to the positions.

Using these properties for the average of (8), the c.m. obeys the equation of a harmonic oscillator,

$$\ddot{\boldsymbol{R}} + \omega_M^2\boldsymbol{R} = \frac{q}{m}\boldsymbol{E}_0(t). \tag{10}$$

Looking at the driven solution in an external field of frequency ω, one immediately arrives at the induced dipole moment $\boldsymbol{d} = -Ne\boldsymbol{R} = \alpha(\omega)\boldsymbol{E}_0$ and the corresponding polarizability

$$\alpha(\omega) = \frac{Ne^2/m}{\omega_M^2 - \omega^2} \tag{11}$$

of the cluster. As in the Rayleigh theory, the Mie resonance occurs at the Mie frequency ω_M.

2.3. Vlasov and fluid models

Another closely related approach treats the electrons of a cluster not as point-particles but in the framework of the kinetic theory by a single-electron distribution function $f(\boldsymbol{r},\boldsymbol{v},t)$ in phase space. The basic kinetic equation for collisionless plasmas is the Vlasov equation

$$\partial_t f(\boldsymbol{r},\boldsymbol{v},t) + \boldsymbol{v}\cdot\partial_{\boldsymbol{r}} f(\boldsymbol{r},\boldsymbol{v},t) - \frac{e}{m}\boldsymbol{E}(\boldsymbol{r},t)\cdot\partial_{\boldsymbol{v}} f(\boldsymbol{r},\boldsymbol{v},t) = 0, \tag{12}$$

where the electric field $\boldsymbol{E}(\boldsymbol{r},t)$ is the sum of the fields produced by the electrons, ions and by the external laser field,

$$\boldsymbol{E} = \boldsymbol{E}_I + \boldsymbol{E}_E + \boldsymbol{E}_0. \tag{13}$$

The first two velocity moments of the distribution function define the particle density n and the mean velocity $\boldsymbol{u}$ according to

$$n = \int d^3v\ f(\boldsymbol{r},\boldsymbol{v},t), \qquad \boldsymbol{u} = \frac{1}{n}\int d^3v\ \boldsymbol{v} f(\boldsymbol{r},\boldsymbol{v},t). \tag{14}$$

Taking the corresponding moments of the Vlasov equation (12) leads in a standard manner to the macroscopic fluid equations

$$\partial_t n + \nabla\cdot(n\boldsymbol{u}) = 0, \tag{15a}$$
$$\partial_t(mn\boldsymbol{u}) + \nabla\cdot(mn\boldsymbol{u}\boldsymbol{u}) = -en\boldsymbol{E} - \nabla\cdot\boldsymbol{P} \tag{15b}$$

with the pressure tensor

$$\boldsymbol{P} = m\int d^3v'\ \boldsymbol{v}'\boldsymbol{v}' f(\boldsymbol{r},\boldsymbol{v},t), \qquad \boldsymbol{v}' = \boldsymbol{v} - \boldsymbol{u}.$$

The equation of motion of the c.m. can be obtained by integrating the momentum equation (15b) over the volume of a concentric sphere surrounding the ion sphere and enclosing all electrons. The particle number and the c.m. are defined by

$$N = \int d^3r\ n, \qquad \boldsymbol{R}(t) = \frac{1}{N}\int d^3r\ n(\boldsymbol{r},t)\boldsymbol{r}. \tag{16}$$

The c.m. velocity can be expressed with the continuity equation (15a) by the fluid velocity

$$\dot{\boldsymbol{R}} = \frac{1}{N}\int d^3r\ \partial_t n\ \boldsymbol{r} = -\frac{1}{N}\int d^3r\ \nabla\cdot(n\boldsymbol{u})\ \boldsymbol{r} = \frac{1}{N}\int d^3r\ n\boldsymbol{u}. \tag{17}$$

The c.m. acceleration therefore is given by

$$\ddot{\boldsymbol{R}} = \frac{1}{N}\int d^3r\ \partial_t(n\boldsymbol{u}) = -\frac{1}{N}\int d^3r\ \frac{e}{m}n\boldsymbol{E} - \nabla\cdot(n\boldsymbol{u}\boldsymbol{u} + \frac{1}{m}\boldsymbol{P}). \tag{18}$$

The divergence term can be transformed by Gauß's law into a surface integral, which vanishes since the fluid variables vanish by assumption on the surface of the integration volume. Using again the actio-reactio-law and assuming further that all electrons stay inside the ion sphere, the average acceleration is given by

$$\ddot{\boldsymbol{R}} = -\frac{e}{Nm}\int d^3r\ n(\boldsymbol{E}_I(\boldsymbol{r}) + \boldsymbol{E}_0(t)) = -\omega_M^2\boldsymbol{R} - \frac{e}{m}\boldsymbol{E}_0(t). \tag{19}$$

There follows again the harmonic oscillator equation (10). From this derivation it follows that the presence of the kinematic and static pressure in the fluid equations does not affect the c.m. motion. Neither do electron-electron collisions in the point-particle model contribute to the c.m. motion. These conclusions are of course dependent on the neglect of surface effects. The Rayleigh and Thomson models are quite general, however, they severely neglect the electron-ion interaction at and beyond the cluster surface. In the following section, we present a simple model of surface scattering that can demonstrate the origin of an additional friction force due to reflections from the surface of the sphere.

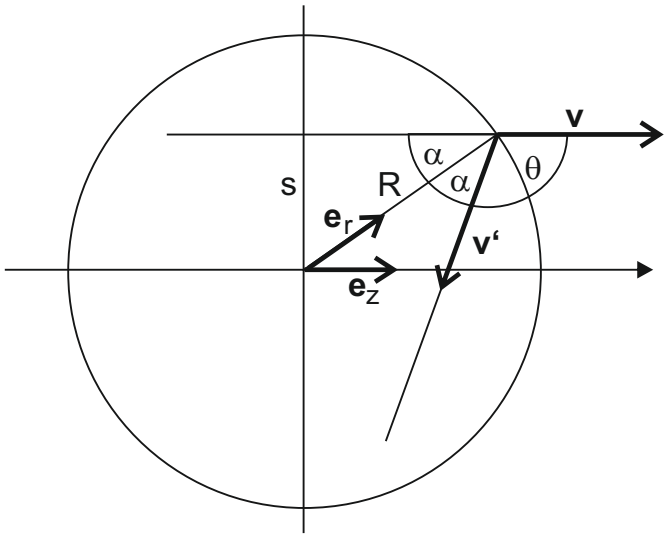

Figure 1. Scattering of a particle at a perfectly reflecting hollow sphere of radius R. The particle is incident with velocity $\boldsymbol{v} = v\boldsymbol{e}_z$ along the z-direction with impact parameter s along a perpendicular direction. The angles of incidence and of reflection are both α. The reflected particle has the velocity $\boldsymbol{v}'$ with $v' = v$, being deflected by an angle θ.

2.4. Hollow-sphere model of surface scattering

The relaxation of Mie oscillations can often be attributed to electron-ion collisions or to collisionless Landau-damping. For larger clusters radiation damping becomes also important. Another cluster-specific relaxation mechanism is due to surface scattering. In this section, we introduce surface scattering by a billiard model. If all electrons remain bounded to the volume of the cluster, one can assume for simplicity an infinitely high potential barrier at the surface of the sphere. We therefore consider a hollow sphere with a perfectly reflecting boundary and derive the friction force due to collisions of free electrons with the cluster surface.

We first assume a beam of particles with a homogeneous density n_0 and a velocity $\boldsymbol{v} = v\boldsymbol{e}_z$ taken along the z-direction. This beam is incident on the inner surface of a hollow sphere as shown in Fig.1. Looking at the reflection of a particle with angle of incidence α, one obtains geometrically the relationship between the impact parameter s and the angle of deflection θ,

$$\theta = \pi - 2\alpha, \qquad s = R\sin\alpha = R\cos(\theta/2). \tag{20}$$

It then follows immediately that the differential cross-section is given by

$$\frac{d\sigma}{d\Omega} = \frac{s}{\sin\theta}\left|\frac{ds}{d\theta}\right| = \frac{1}{4}R^2. \tag{21}$$

It is equal to the more familiar differential cross section for scattering at the outside surface of a hard sphere. The total cross-section becomes $\sigma_T = \pi R^2$ and corresponds to the maximum circular cross-section of the sphere.

The rate of momentum change due to surface collisions can be calculated in terms of the momentum transfer $\Delta\boldsymbol{p}$ for a single collision and the scattering rate $j d\sigma$ as

$$\frac{\Delta\boldsymbol{p}}{\Delta t} = \int \Delta\boldsymbol{p}(s,\phi) j d\sigma = \int d\Omega\ \Delta\boldsymbol{p}(\theta,\phi)\ j\frac{d\sigma}{d\Omega}, \qquad j = n_0 v. \tag{22}$$

During the reflection at the surface, the normal component of the momentum becomes reversed. Writing the momenta $\boldsymbol{p}$ of the incident and $\boldsymbol{p}'$ of the reflected particles as a sum of outward directed normal (r) and tangential (t) components, one obtains

$$\boldsymbol{p} = \boldsymbol{p}_t + \boldsymbol{p}_r, \qquad \boldsymbol{p}' = \boldsymbol{p}_t - \boldsymbol{p}_r, \qquad \Delta\boldsymbol{p} = -2\boldsymbol{p}_r = -2\boldsymbol{p}\cdot\boldsymbol{e}_r\boldsymbol{e}_r. \tag{23}$$

In spherical coordinates the angle dependence of the momentum change can be expressed as

$$\Delta\boldsymbol{p} = -2mv\cos\alpha \begin{pmatrix} \sin\alpha\cos\phi \\ \sin\alpha\sin\phi \\ \cos\alpha \end{pmatrix} = -mv \begin{pmatrix} \sin\theta\cos\phi \\ \sin\theta\sin\phi \\ 1-\cos\theta \end{pmatrix}. \tag{24}$$

Integrating now (24) over the solid angle, all angle-dependent parts average to zero. The only nonvanishing contribution comes from the constant term in the z-component. It yields

$$\frac{\Delta\boldsymbol{p}}{\Delta t} = j\frac{d\sigma}{d\Omega}\int d\Omega\ \Delta\boldsymbol{p} = -n_0 v\sigma_T\ m\boldsymbol{v}. \tag{25}$$

The average rate of momentum change per particle is a velocity dependent friction force

$$\boldsymbol{F}(\boldsymbol{v}) = \frac{1}{N}\frac{\Delta\boldsymbol{p}}{\Delta t} = -\nu(v)m\boldsymbol{v}, \qquad \nu(v) = \frac{3}{4}\frac{v}{R}. \tag{26}$$

Note that the friction coefficient $\nu(v)$ is velocity dependent and that it scales with $1/R$ with the cluster radius. This scaling arises basically from the surface to volume ratio of $\sigma_T/N \propto 1/R$.

Next, we consider an equilibrium with a spatially homogeneous electron density and an arbitrary isotropic velocity distribution $f(\boldsymbol{v}) = n_0 g(v)$ inside the hollow sphere. The distribution function $f(\boldsymbol{v})$ is normalized to the number of particles N within the sphere and therefore

$$\int d^3v\ g(v) = 1. \tag{27}$$

For example, a Fermi distribution has equal weights of all occupied velocity points and is given by

$$g(v) = \frac{3}{4\pi v_F^3}\theta(v_F - v), \tag{28}$$

where the maximum velocity v_F denotes the Fermi-velocity.

The total friction force due to surface reflections then is given by an integral over velocity space,

$$\langle\boldsymbol{F}(\boldsymbol{v})\rangle \equiv \int d^3v\ g(v)\boldsymbol{F}(\boldsymbol{v}). \tag{29}$$

Since $g(v)\boldsymbol{F}(\boldsymbol{v})$ is a central field, the velocity integral vanishes and the friction force is zero. Exciting now a Mie oscillation with velocity $\dot{\boldsymbol{R}}(t)$ inside the cluster, all electrons will be shifted to the new velocity $\boldsymbol{v}' = \boldsymbol{v} + \dot{\boldsymbol{R}}$ and they experience the friction force $\boldsymbol{F}(\boldsymbol{v}')$. Integrating now over all particles yields a nonvanishing average

$$\boldsymbol{F}_M = \langle\boldsymbol{F}(\boldsymbol{v}')\rangle = -\frac{3m}{4R}\langle|\boldsymbol{v}+\dot{\boldsymbol{R}}|(\boldsymbol{v}+\dot{\boldsymbol{R}})\rangle. \tag{30}$$

Since the Mie oscillation is considered a small perturbation, the average is only calculated to first order in $\dot{\boldsymbol{R}}$. Setting $\boldsymbol{v} = v\boldsymbol{n}$ and $\dot{\boldsymbol{R}} = \dot{R}\boldsymbol{e}_z$ one has to first order $v' = v + \boldsymbol{n}\cdot\boldsymbol{e}_z\dot{R}$ and

$$v'\boldsymbol{v}' = v\boldsymbol{v} + \boldsymbol{v}\boldsymbol{n}\cdot\dot{\boldsymbol{R}} + v\dot{\boldsymbol{R}} = v^2\boldsymbol{n} + \boldsymbol{n}\boldsymbol{n}\cdot\boldsymbol{e}_z v\dot{R} + v\dot{\boldsymbol{R}}\ . \tag{31}$$

Integrating over the solid angle in velocity space yields

$$\int d\Omega\ \boldsymbol{n} = 0, \qquad \int d\Omega\ \boldsymbol{nn} = \frac{4\pi}{3}\boldsymbol{I}, \tag{32}$$

where $\boldsymbol{I}$ denotes the unit tensor. Using these properties, the remaining integral over the radial coordinate v becomes

$$\langle v'\boldsymbol{v}'\rangle = \frac{16\pi}{3}\dot{\boldsymbol{R}}\int_0^\infty dv\ v^3 g(v). \tag{33}$$

Finally, choosing the Fermi distribution (28), the velocity average becomes $\langle v'\boldsymbol{v}'\rangle = v_F\dot{\boldsymbol{R}}$ and the friction force (30) is given by

$$\boldsymbol{F}_M = -\nu m\dot{\boldsymbol{R}}, \qquad \nu = \frac{3}{4}\ \frac{v_F}{R}. \tag{34}$$

Comparing with the single-beam result (26), one can see that the force is now linear in the velocity perturbation $\dot{\boldsymbol{R}}$ and that the friction coefficient is evaluated at the Fermi-velocity. Adding this surface-friction force to the center of mass motion yields the damped harmonic oscillator equation

$$\ddot{\boldsymbol{R}} + \nu\dot{\boldsymbol{R}} + \omega_M^2\boldsymbol{R} = -\frac{e}{m}\boldsymbol{E}_0(t). \tag{35}$$

The decay of an initial perturbation can be defined by the solution to the homogeneous equation ($\boldsymbol{E}_0 = 0$). Assuming an exponential time-dependence $\propto e^{-i\omega t}$ yields complex eigenfrequencies

$$\omega_{1,2} = \pm\sqrt{\omega_M^2 - \left(\frac{\nu}{2}\right)^2} - i\frac{\nu}{2}. \tag{36}$$

and for $\omega_M > \nu/2$ a decay rate of

$$\gamma = \frac{\nu}{2} = A\ \frac{v_F}{2R}, \qquad A = \frac{3}{4}. \tag{37}$$

The exponential decay rate corresponds to a Lorentzian line shape with a full width at half maximum (FWHM) of $\Delta\omega = 2\gamma$.

The surface plasmon decay rate was considered by a number of authors under various assumptions and with slightly different results. A classical approach has been based on the estimate of the mean free path L within finite-size particles. For a sphere, the authors obtain $L = R$ for isotropic [2] and $L = \frac{4}{3}R$ for diffuse scattering [17, 3]. The effective collision frequency was then estimated as

$$\nu = v_F/L = A\frac{v_F}{R} \tag{38}$$

with $A = 1$ or $A = 3/4$, respectively. The present result (37) shows the same scaling and even agrees with the $L = \frac{4}{3}R$ model. However, one should notice that the average mean free path is determined geometrically, while the present scattering model is a kinetic approach based on particle dynamics, specular reflection and the velocity distribution function. Plasmon damping in metal particles was also considered quantum theoretically [4, 18, 19, 5]. In a thorough review of the early work, it was concluded that [5]

$$A = p\ \sqrt{1 + \frac{\omega}{E_F}}, \tag{39}$$

where $p = 3/4$ in quasi-classical and $p = 3/\pi^2$ in random-phase approximation (RPA). The dependence on the excitation frequency ω derives from resonances with quantum-mechanical

excitation energies of various dipole transitions. Because of this quantum correction, the quasi-classical result is somewhat larger than the classical estimate (37). The more complete RPA treatment leads to a smaller coefficient. For silver particles ($E_F \approx 5.5$ eV, $\omega \approx 3$ eV) the frequency-dependent factor is about 1.25. In this case the FWHM line widths become $\Delta\omega = 0.94\ v_F/R$ for the semi-classical and $\Delta\omega = 0.38\ v_F/R$ for the RPA case. Both approximations proved to be well consistent with different experimental results [17, 20, 5]. In later experiments, higher absorption values have been attributed to embedding or substrate materials while a smaller value of $A = 0.25$ was measured for free isolated Ag [16] and Au [21, 22] clusters. The classical approach (37) yields a somewhat larger value $A = 0.75$, which may be viewed as a reasonable order of magnitude estimate. A discussion of surface damping under various conditions can be found in [16, 23, 24].

3. Particle simulations

3.1. Computational model

To study the surface damping effects in more detail, we have performed particle simulations of N electrons interacting with a fixed homogeneous ion sphere. The ion sphere has radius R and charge Ne, where e denotes the positive elementary charge. The average electron density is $n_0 = 3N/(4\pi R^3)$ and the mean particle distance r_s can be defined by $4\pi n_0 r_s^3/3 = 1$. It is convenient to introduce dimensionless positions $\boldsymbol{r}' = \boldsymbol{r}/r_s$, times $t' = \omega_M t$ and electric fields $\boldsymbol{E}' = e\boldsymbol{E}/(m\omega_M^2 r_s)$, where ω_M is the Mie frequency (6). Omitting the prime for simplicity of notation, the dimensionless equations of motion for an electron with charge $q = -e$ becomes,

$$\ddot{\boldsymbol{r}}_i = -\boldsymbol{E}_0(t) - \boldsymbol{E}_I(\boldsymbol{r}_i) - \sum_{j\neq i} \boldsymbol{E}_E(\boldsymbol{r}_i - \boldsymbol{r}_j), \qquad i = 1, \cdots, N. \tag{40}$$

Here $\boldsymbol{E}_0(t)$ denotes an external laser field and $\boldsymbol{E}_I$ the electric field of the ion sphere that is given by

$$\boldsymbol{E}_I(\boldsymbol{r}) = \boldsymbol{r}\left(\theta(R-r) + \theta(r-R)\frac{R^3}{r^3}\right). \tag{41}$$

The electron-electron interaction $\boldsymbol{E}_E$ will be modelled by a softcore Coulomb potential and a corresponding electric field,

$$\phi(\boldsymbol{r}) = -\frac{1}{\sqrt{r^2+\epsilon^2}}, \qquad \boldsymbol{E}_E(\boldsymbol{r}) = -\nabla\phi(\boldsymbol{r}) = -\frac{\boldsymbol{r}}{(r^2+\epsilon^2)^{3/2}}. \tag{42}$$

A constant $\epsilon = 2$ is used in the simulations to eliminate hard collisions with impact parameters near and below the interparticle distance r_s. Apart from this constant, the equations of motion (40) contain only a single parameter, which is the dimensionless radius $R = N^{1/3}$ of the sphere.

The equations of motion have to be supplemented by initial conditions. Initially, the electrons are placed at random positions inside the sphere. The velocities are chosen with random directions and the kinetic energies are distributed according to the Fermi distribution (28). The Fermi energy E_F defines another dimesionless parameter of the model, which is the coupling parameter $\Gamma = e^2/(r_s E_F))$ of the plasma. In the present calculations, we have always chosen a weakly coupled plasma with $\Gamma = 0.1$. The radius R is varied in the range $20 - 30$, corresponding to particle numbers between 8000 and 27000.

3.2. Results

We now discuss some of the results of the present particle simulations for a cluster with dimensionless radius $R = 28$ and coupling parameter $\Gamma = 0.1$. To study the evolution of the Mie plasmon and its damping, the electron ensemble is initially rigidly shifted by a displacement

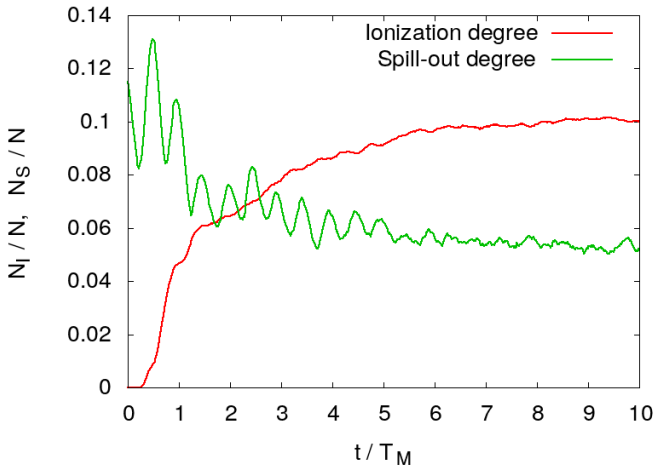

Figure 2. Evolution of the spill-out degree and the outer-ionization degree over 10 Mie periods. In an initial phase of approximately $4-5$ Mie periods, the outer-ionization degree rises and subsequently reaches a quasi-stationary regime. The initial spill-out degree corresponds to the initial shift of the particles with respect to the ion sphere. The spill-out degree initially oscillates with twice the Mie frequency, since electrons are ejected in both maxima of one Mie oscillation. Finally, it also approaches some quasi-stationary regime. ($R = 28$, $\Gamma = 0.1$, $\Delta x = 0.15R$)

$\Delta x = 0.15R$ from the equilibrium configuration. The evolution of the mean velocity of the electrons then indicates exponentially damped Mie oscillations. In contrast to the simplified models of Sec. 2, the electrons can reach and cross the cluster surface. To demonstrate electron spill out and outer ionization of the cluster, we have defined a spill-out degree as the fraction of particles in a shell $R < r < 1.5R$ and an outer-ionization degree as the fraction of particles in the exterior region $r > 1.5R$. Fig. 2 shows the evolution of both parameters over the simulation time of 10 Mie periods $T_M = 2\pi/\omega_M$. It can be seen that electrons are ejected in each half wave of the Mie oscillation, leading finally to an outer-ionization degree of about 10 %. The present simulation model does not allow to lower the ionization degree well below the 1 % level. The present initial ensemble is no perfect equilibrium and one therefore has to accept some outer ionization even without perturbation.

The approach to a quasi-stationary regime can also be recognized in the evolution of the particle energies. In Fig. 3, one can recognize the mean kinetic energy per particle $W = \frac{1}{2}\overline{v^2}$ and the temperature T defined by $\frac{3}{2}T = \frac{1}{2}\overline{(v-\overline{v})^2}$. The initial Fermi energy $E_F = 1/\Gamma = 10$ corresponds to the mean energy $W = (3/5)E_F = 6$ and the temperature $T = \frac{2}{3}W = 4$. While the kinetic energy of the mean velocity decreases, the temperature increases and becomes nearly constant in the quasi-stationary regime.

The evolution of the potential energies of the electrons can be seen in Fig. 4. The electron-ion potential is the energy of all electrons in the potential of the ion sphere per particle, the electron-electron potential is the interaction energy of all electron pairs per particle. We have also convinced that the total energy consisting of the kinetic energy and the potential energies is very well conserved in the calculations up to the accuracy of the finite-difference scheme. The potential energies decrease in magnitude due to the expansion of the electron cloud. Noting the different scales of the axes, this decrease is naturally much larger in the ionization regime shown in (a),(c) than in the final quasi-stationary regime (b),(d). Looking at the oscillation frequencies of the potential energies, one can observe a decrease from $2\omega_M$ to frequencies in the

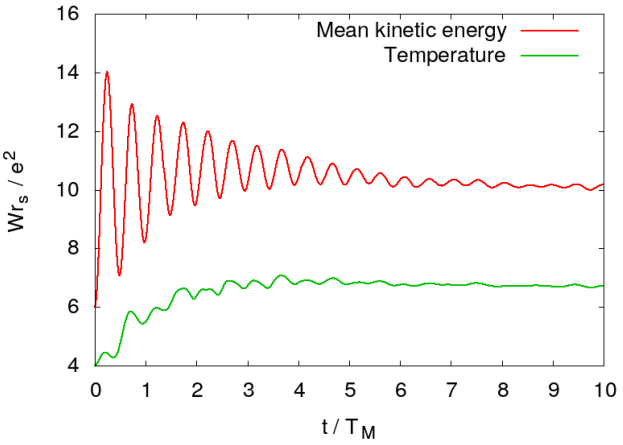

Figure 3. Evolution of the mean kinetic energy and the temperature. In the initial phase, the kinetic energy of the Mie oscillation is gradually converted into temperature. In the final stage of the evolution, no further heating is observed and the temperature remains nearly constant. ($R = 28$, $\Gamma = 0.1$, $\Delta x = 0.15R$)

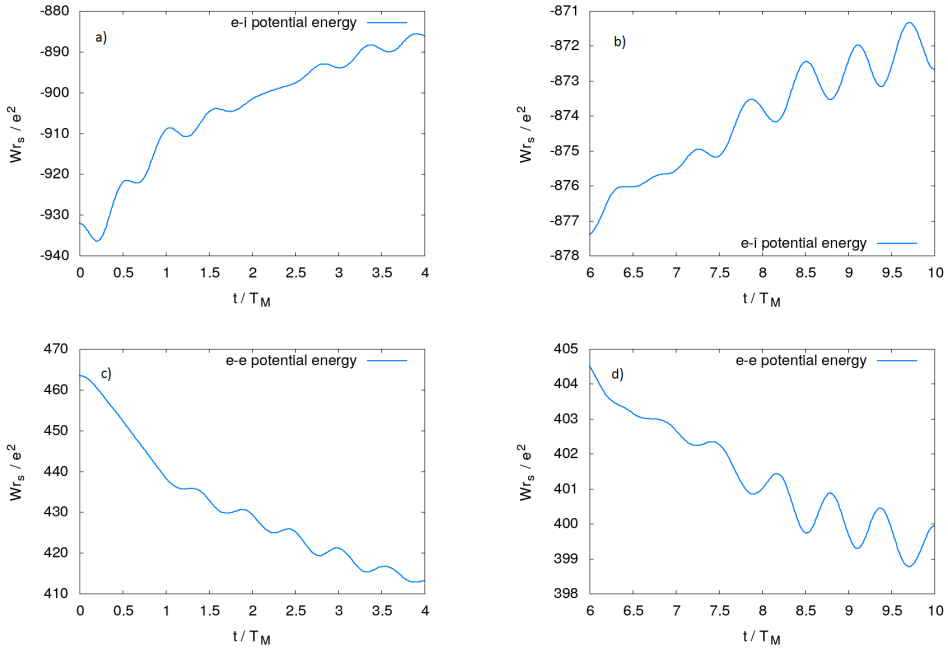

Figure 4. Evolution of potential energies. The magnitude of the potentials decreases due to the increase of the extension of the electron cloud. Furthermore, a decrease of the oscillation frequency indicates a conversion from surface modes with frequency $2\omega_M$ to volume modes with frequencies in the range of ω_p. a) Initial and b) final stage of the electron-ion potential energy. c) Initial and d) final stage of the elelctron-electron potential energy. ($R = 28$, $\Gamma = 0.1$, $\Delta x = 0.15R$)

range of ω_p and opposite phases in the electron-electron and electron-ion potentials. This shift indicates a conversion from surface to volume modes that has been observed in recent quantum calculations of plasmon decay [1]. The phase difference also indicates radial oscillations of the electron density inside the ion sphere where a compression increases the electron repulsion but decreases the ion attraction. Although the mode conversion process has been demonstrated much more convincingly in the quantum regime, the present classical particle simulations can confirm a similar behaviour in the quasi-stationary regime following the ionization stage.

For sufficiently large clusters, we have observed an exponential decay of the Mie oscillations. Using again the preceeding parameters, the oscillation and the decay of the mean velocity V is shown in Fig. 5. The damped oscillation can be very well fitted to the function

$$V(x) = a\sin(\omega t + p)e^{-\gamma t} + c \tag{43}$$

with fit parameters a, ω, p, γ and c. The constant c accounts for a small drift velocity. The fit is applied both to the initial and final phases as indicated in Fig. 5. In this manner, one can define a maximum and a minimum decay rate γ corresponding to the initial ionization phase and the final quasi-stationary phase, respectively. These decay rates have been evaluated as a function of the cluster radius in the range $R = 20$ up to $R = 30$ as shown in Fig. 6. The decay rates follow roughly the expected $1/R$ scaling of (37), however, the deviations from this simple law are appreciable. We attribute the scattering of the data to a mixture of various decay mechanisms including collisional damping, ionization damping, surface damping and damping by mode conversion. The calculated decay rates are well consistent with previous models. Evaluating for instance the damping constant A in (37) for $\tilde{\gamma} = 2\pi\gamma \approx 0.2 - 0.4$, $R = 25$ and with an approximate Fermi energy of $E_F = \frac{5}{3}W \approx 15$ in the final stationary phase, one obtains

$$A = \frac{2R}{v_F}\gamma = \frac{2R}{\sqrt{2E_F}}\frac{\tilde{\gamma}}{2\pi} \approx 0.3 - 0.6. \tag{44}$$

This range of values is close to commonly accepted decay constants as discussed below (39).

4. Conclusions

We have investigated the decay of Mie oscillations in spherical clusters by classical particle simulations. In appropriate units, the physical model contains only two physical parameters namely the cluster radius $R = N^{1/3}$ and the plasma coupling parameter $\Gamma = e^2/(r_s E_F)$. We have restricted attention to the weakly coupled regime, setting $\Gamma = 0.1$. For sufficiently large clusters with radii larger than 20, we observed an exponential decay of the Mie oscillations. The decay rate has been calculated in the range $R = 20$ up to $R = 30$, where a calculation of the electron-electron interaction was computationally feasible. For larger clusters, the computational effort of calculating pairwise particle interactions increases strongly and one has to resort to other methods. The decay constants proved in the expected range of values, although considerable deviations from the simple scaling law (39) have been observed. We conclude that a mixture of different damping processes including outer ionization, collisional damping, surface damping and mode conversion may contribute. Outer ionization could not be completely suppressed most likely due to an imperfect equilibrium state. Collisional damping depends on the parameter ϵ of the soft-core potential. Decreasing its value the damping constant has increased. This shows that one is not in a perfect collisionless regime. Surface damping is likely to play a dominant role since we obtained close quantitative agreement with the corresponding scaling law and have observed the related mode conversion process described in [1]. Plasma-wave dynamics in the interior of the cluster has also been observed in previous particle simulations of laser-excited clusters [25, 26].

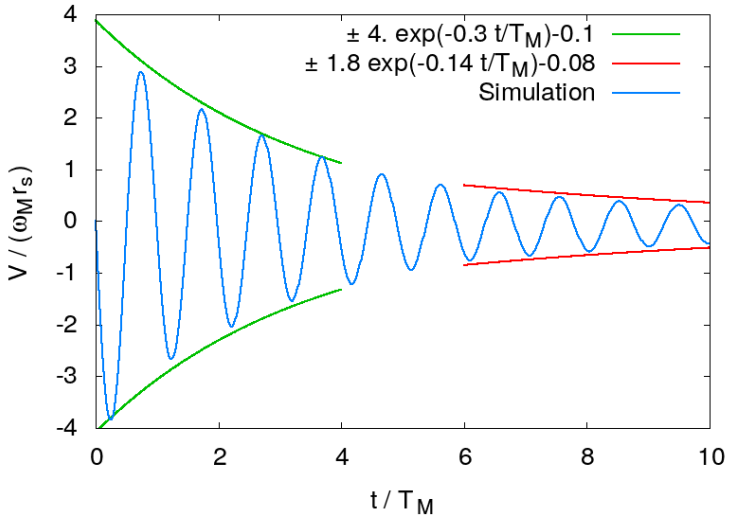

Figure 5. Mie oscillation of the mean velocity V and exponential decay laws in the initial and final stages of the calculation. ($R = 28$, $\Gamma = 0.1$, $\Delta x = 0.15R$)

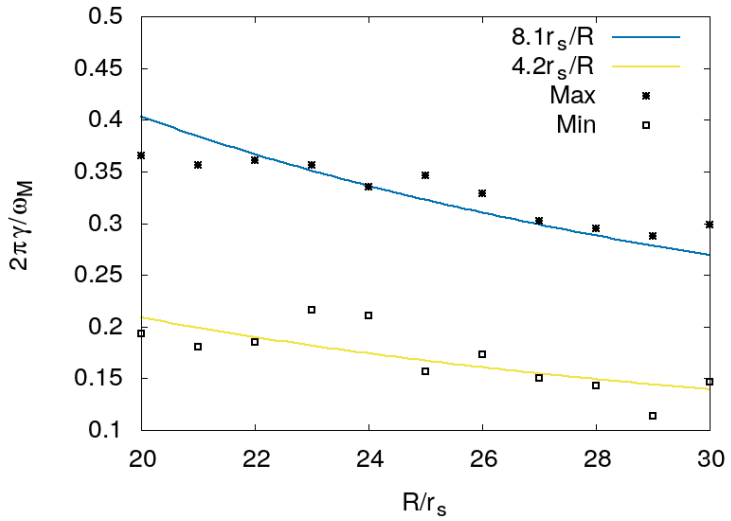

Figure 6. Decay rate γ of Mie oscillations as a function of the cluster radius R. The maximum rate corresponds to the first four periods, the minimum rate to the last four periods considered. Both rates are compared to $1/R$ fitting functions. ($R = 20 - 30$, $\Gamma = 0.1$, $\Delta x = 0.15R$)

[1] El-Khawaldeh A and Kull H J 2017 *Phys. Rev. A* **95**(4) 043401
[2] Euler J 1954 *Z. Phys.* **137** 318
[3] Coronado E A and Schatz G C 2003 *J. Chem. Phys.* **119** 3926–3934
[4] Kawabata A and Kubo R 1966 *J. Phys. Soc. Jpn.* **21** 1765
[5] Thoai D T and Ekardt W 1982 *Solid State Commun.* **41** 687 – 690
[6] Greschik F, Arndt L and Kull H J 2005 *EPL (Europhys. Lett.)* **72** 376–382
[7] Petrov G M and Davis J 2006 *Phys. Plasmas* **13** 033106
[8] Ditmire T, Donnelly T, Rubenchik A M, Falcone R W and Perry M D 1996 *Phys. Rev. A* **53** 3379–3402
[9] Döppner T, Fennel T, Diederich T, Tiggesbäumker J and Meiwes-Broer K H 2005 *Phys. Rev. Lett.* **94**(1) 013401
[10] Mikaberidze A, Saalmann U and Rost J M 2008 *Phys. Rev. A* **77**(4) 041201
[11] Fomichev S V, Popruzhenko S V, Zaretsky D F and Becker W 2003 *J. Phys. B* **36** 3817
[12] Kundu M and Bauer D 2006 *Phys. Rev. Lett.* **96**(12) 123401
[13] Mulser P, Bauer D and Ruhl H 2008 *Phys. Rev. Lett.* **101**(22) 225002
[14] Lord Rayleigh FRS 1897 *The London, Edinburgh, and Dublin Philosophical Magazine and Journal of Science* **44:266** 28–52
[15] Thomson J J FRS 1904 *The London, Edinburgh, and Dublin Philosophical Magazine and Journal of Science* **7:39** 237–265
[16] Hövel H, Fritz S, Hilger A, Kreibig U and Vollmer M 1993 *Phys. Rev. B* **48**(24) 18178–18188
[17] Kreibig U 1974 *J. Phys. F: Met. Phys.* **4** 999
[18] Lushnikov A A and Simonov A J 1974 *Z. Phys.* **270** 17–24
[19] Lozovik Y E and Nishanov V N 1978 *Sov. Phys. Solid State* **20(12)** 2111
[20] Abe H, Schulze W and Tesche B 1980 *Chem. Phys.* **47** 95 – 104
[21] Berciaud S, Cognet L, Tamarat P and Lounis B 2005 *Nano Lett.* **5** 515–518
[22] Novo C, aand Jorge Perez-Juste D G, Zhang Z, Petrova H, Reismann M, Mulvaney P and Hartland G V 2006 *Phys. Chem. Chem. Phys.* **8** 3540–3546
[23] Gildenburg V B, Kostin V A and Pavlichenko I A 2011 *Phys. Plasmas* **18** 092101
[24] Juvé V, Cardinal M F, Lombardi A, Crut A, Maioli P, Pérez-Juste J, Liz-Marzán L M, Del Fatti N and Vallée F 2013 *Nano Lett.* **13** 2234–2240
[25] Greschik F and Kull H-J, 2004 *Laser and Particle Beams* **22** 137–145
[26] Varin C, Peltz C, Brabec T and Fennel T. 2012 *Phys. Rev. Lett.* **108** 175007